Mine Water and the Environment (2023) 42:293–311
https://doi.org/10.1007/s10230-023-00937-3

TECHNICAL ARTICLE

Establishing Geomorphic Reference Criteria for Design of River Diversions Around Mine Pits in the Pilbara, Western Australia

Alissa Flatley[1] · **Ian Rutherfurd**[1,2]

Received: 8 August 2022 / Accepted: 17 May 2023 / Published online: 9 June 2023

Abstract
The poor condition of river diversion channels can prevent mining companies from relinquishing their mine to the government after mining has ceased. Many regions lack a locally derived template for integrating appropriate geomorphic and hydraulic conditions from unmodified river channels into river diversion designs to help guide post-mining closure activities. Establishing baseline geomorphic reference criteria for unmodified catchments can guide restoration efforts to allow recovery and stability of the fluvial system. Design-wise, channels should be built so that flow conditions are able to move sediment, but not high enough to accelerate erosion in the channel. We used natural headwater channels to inform a regional guide for geomorphic criteria for artificial channels constructed in the Pilbara, Western Australia. We provide guideline hydraulic criteria for specific channel types, including velocity, stream power, and bed shear stress values for five key channel types: alluvial single thread (≥ cobble) and single thread (sand), bedrock/confined channel sections, island-barform channels, and heavily vegetated channels.

Keywords Mining · River channel · River relocation · River restoration · Mine closure

Introduction

Many engineering projects involve relocating stream channels into an artificial channel for part of their length (Flatley et al. 2018). These are known as river diversions and are particularly common at mines where streams are diverted around large, open-cut mine pits. There are hundreds of such diversions around mines in Australia, and each has been constructed with a varying degree of effort to mimic a natural river channel (White et al. 2014a, b). There are many challenges in designing these diversion channels, but one specific problem is how they are treated in the process of mine closure, when mining has finished, and the objective is site rehabilitation and relinquishment.

Most mine closure plans prioritise a 'natural' ecosystem as a preferred end land use (Hine and Erskine 2016; Lamb et al. 2015). River diversions can adversely affect the environment for thousands of years, and so they are of concern to regulators. River diversions generally suffer from a lack of vegetation establishment, along with channel erosion and enlargement (Dragicevic et al. 2012), consequent upstream erosion (Erskine 2006), hanging tributary incision, and geomorphic processes that do not best replicate natural channels (White and Hardie 2000). There is an overall lack of sediment deposition in most channels, with sediment size not reflective of natural counterparts due to continuity issues such as culvert placement, increased channel dimensions (White et al. 2014a, b), reduced channel roughness, greater slopes, and heightened channel stream power during flood flows (Flatley and Markham 2021). In this paper, we focus on the design of diversion channels around iron-ore mine pits in the Pilbara region of Western Australia. We suggest that the natural characteristics of creeks and streams in the vicinity of the mine can provide valuable targets for design of these diversion channels, and eventually, criteria for mine closure.

Ninety percent of Australia's identified iron ore resources are in the Pilbara region (Fig. 1), supporting some of the largest mining sites in the world (Geoscience Australia 2015). Eighty percent of this total iron ore yield is found

✉ Alissa Flatley
Alissa.flatley@unimelb.edu.au

[1] School of Geography, Earth and Atmospheric Sciences, University of Melbourne, Parkville, Melbourne, VIC 3010, Australia

[2] Alluvium Consulting, 105 Dover Street, Cremorne, VIC 3121, Australia

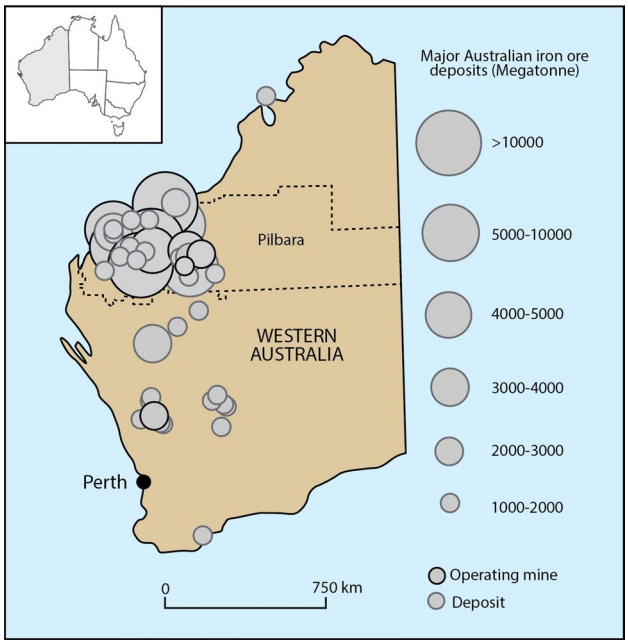

Fig. 1 Map of mining areas in Western Australia with the Pilbara region, outlined. Modified from Geoscience Australia (2016)

within the Hamersley Basin, a region located in the southern part of the Pilbara Craton (Li et al. 1993). There has been a large increase in the number of mines targeting channel iron deposits (CID), located in palaeochannels typically below the groundwater table (Atkinson et al. 2017). Smaller watercourses (with catchments < 1 km^2) were previously allowed to flow into mining pits, but now this practice has been recognised as a risk to surface water management and more effort has been made to divert, reinstate, and protect these small river channels (Atkinson et al. 2017; Flatley and Markham 2021).

Generally, Australia has a poor record on mine closure, with 75% of Australian mines undergoing premature or unplanned closure, resulting in unsatisfactory shutting, mine abandonment, or poor mine rehabilitation (Laurence 2006; Roche and Judd 2016). The arid and semi-arid climatic setting of many Australian mines can create additional challenges for mining development and closure (Conesa et al. 2006; Khademi et al. 2018), including the effects of extreme climatic events with respect to water balance and surface water management (Van Zyl Dirk and Straskraba 1999).

There is increasing expectations that artificial river diversion channels should eventually mimic their natural counterparts (Flatley et al. 2018; Grace et al. 2014; White and Hardie 2000). Whilst mining companies have many criteria for the design and construction of diversions (including cost, flood capacity, stability), we are concerned here with the criteria for river channels post-mining, during the mine closure and rehabilitation phase. Mine closure criteria are typically identified by establishing an underlying objective (referring to a written statement declaring a specific target to be achieved) and criteria, referring to a list of quantitative and measurable benchmarks required to achieve the outlined objective (Coppin 2013). Examples of underlying objectives for river diversions include the need for diversions to be stable, with a natural rate of channel change. River diversions should also be self-sustaining and include geomorphic and vegetation features similar to regional watercourses (Fig. 2). They should also positively contribute to river health values and impose no long-term liability on the state, the proponent, or the community (State of Queensland 2019).

To meet the closure objectives for river diversion channels, specific hydraulic criteria have been developed to provide a template for the derivation of closure criteria and to improve the sustainable design of these channels before mine closure. In Queensland, the Australian Coal Association Research Program (ACARP) criteria were created to establish guideline hydraulic and geomorphic design criteria for regional watercourses to establish the ideal range of hydraulic conditions within natural river channels in the Bowen Basin, Queensland (State of Queensland 2019; White and Hardie 2000). Hydraulic values were presented for frequent and rare flows, with stream types defined by whether they are alluvial (with high or low sediment supply) or bedrock controlled (White et al. 2014a, 2014b). Elsewhere, in areas such as the Pilbara, Western Australia and the Northern Territory, there is a shortage of government policy, design guidelines, or closure criteria for these final fluvial landforms (Erskine 2006). This lack of guidance presents a major barrier to facilitating the relinquishment of the mine site post-closure and contributes to many long-term rehabilitation challenges (Flatley and Markham 2021). There is only a small amount of research on design criteria for river diversions, and even less that focuses on streams in the Pilbara, hence the rationale for this investigation. Our aim is to better describe the geomorphic and hydraulic character of those streams as a basis for designing the diversion channels through the development of design criteria.

In this paper, we establish hydraulic and geomorphic characteristics or small headwater river channels in the Pilbara. These characteristics are developed using 2D modelling for five distinct headwater channel types across a range of flow return intervals. These values provide quantitative benchmarks to best replicate natural channel conditions within river diversion channels and can provide guideline criteria against which diversion channels can be judged when it comes to relinquishment. After describing the study sites in the Pilbara, we outline the approach to the study.

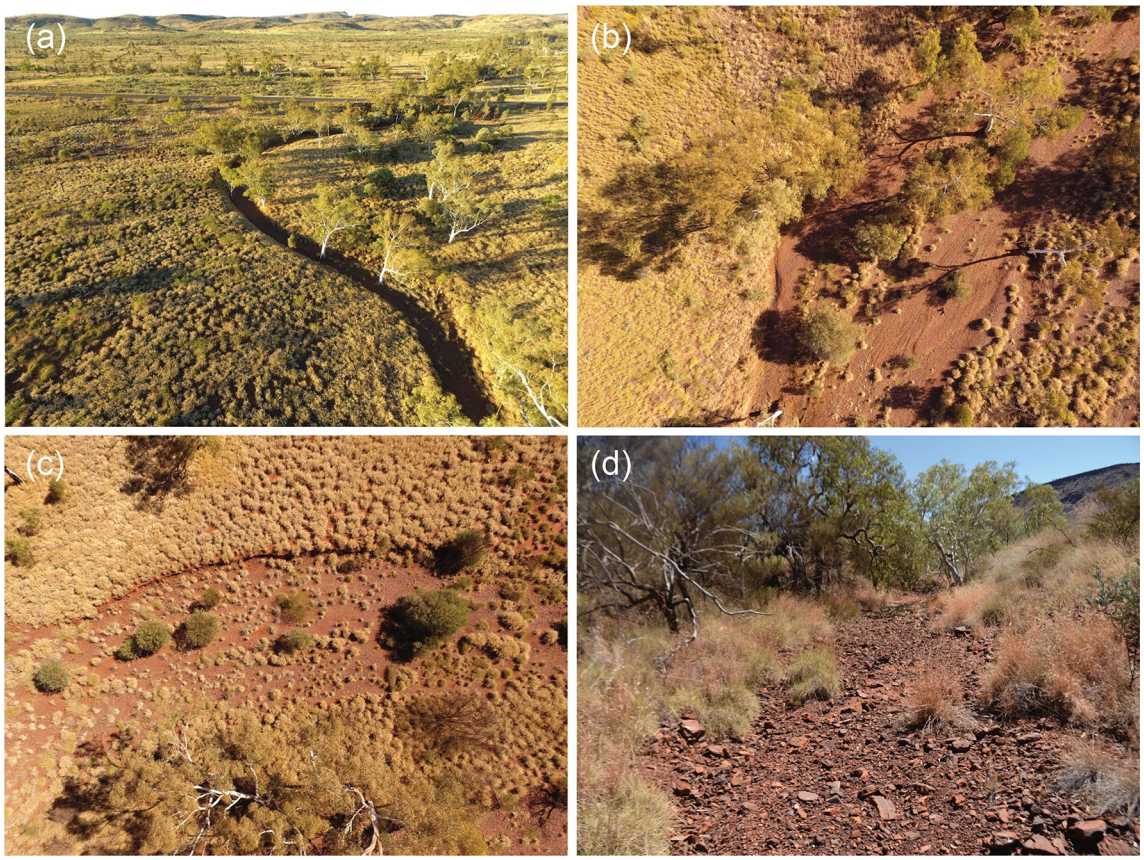

Fig. 2 Examples of headwater river channels in the Pilbara, WA: **a** aerial view of small cobble single thread channel, **b** island barform with trees, **c** nascent barforms in a vegetated channel, **d** narrow single channel dominated by cobble bedload

Study Area

The focus of this study was the Yandi iron-ore mine site located on Marillana Creek, in the Fortescue catchment in the Pilbara, Western Australia (Fig. 3). The Pilbara is an arid to semi-arid region with ephemeral river flow that is seldom gauged. Surface water is highly variable and limited within the region (Johnson and Wright 2003). Rainfall averages about 334 mm/yr, with the Hamersley Ranges receiving elevated annual rainfall and lower potential evaporation (Charles et al. 2015). The focus here were a series of headwater channels that join Marillana Creek, the largest river flowing through the Yandi Mine site. Marillana Creek has a total catchment area of 2230 km^2 (Rio Tinto 2010) and flows eastward through the downstream Rio Tinto Yandicoogina mine. Marillana Creek joins Weeli Wolli Creek, which flows northward before draining into the Fortescue Valley and Fortescue River (Johnson and Wright 2003; Rio Tinto 2010).

The Pilbara landscape is ancient and has an iron-rich lithology. The surface regolith is characterised by bedrock outcrops and variable residual (e.g. laterite) and colluvial regolith cover. The armouring capabilities of this surface regolith have been identified in addition to the presence of erosion-resistant ferricretes and iron rich-duricrusts (canga) (Cooke et al. 1993). Broad regional studies on the surface drainage patterns and regolith have been carried out by Churchward and McArthur (1980) and McKenzie et al. (2009). Regional geodiversity and endemism has been reported by Pepper et al. (2013) alongside studies of groundwater recharge within the ephemeral streams that also describe catchment physiography (Dogramaci et al. 2015) and hydrology (Charles et al. 2015; RioTinto 2010).

The Yandi mine is located in the Marillana Formation, a geological unit comprised of various sediments occupying the paleochannel of Marillana Creek and its adjoining tributaries. The Marillana formation is estimated to host a resource totalling more than 4000 Mt of channel iron deposits (CID; Ramanaidou et al. 2003). CID is comprised of a complex and heterogenous mix of coarse sand- and gravel-sized pisolitic deposits, which have been cemented into a goethite matrix (Ramanaidou et al. 2003; Rio Tinto 2010). To facilitate mining of the CID, many small channels have been diverted around the mine site. These minor ungauged tributaries were the focus of this investigation. The tributary channels in this study vary from bedrock or alluvial single thread channels to an alluvial multithread channel

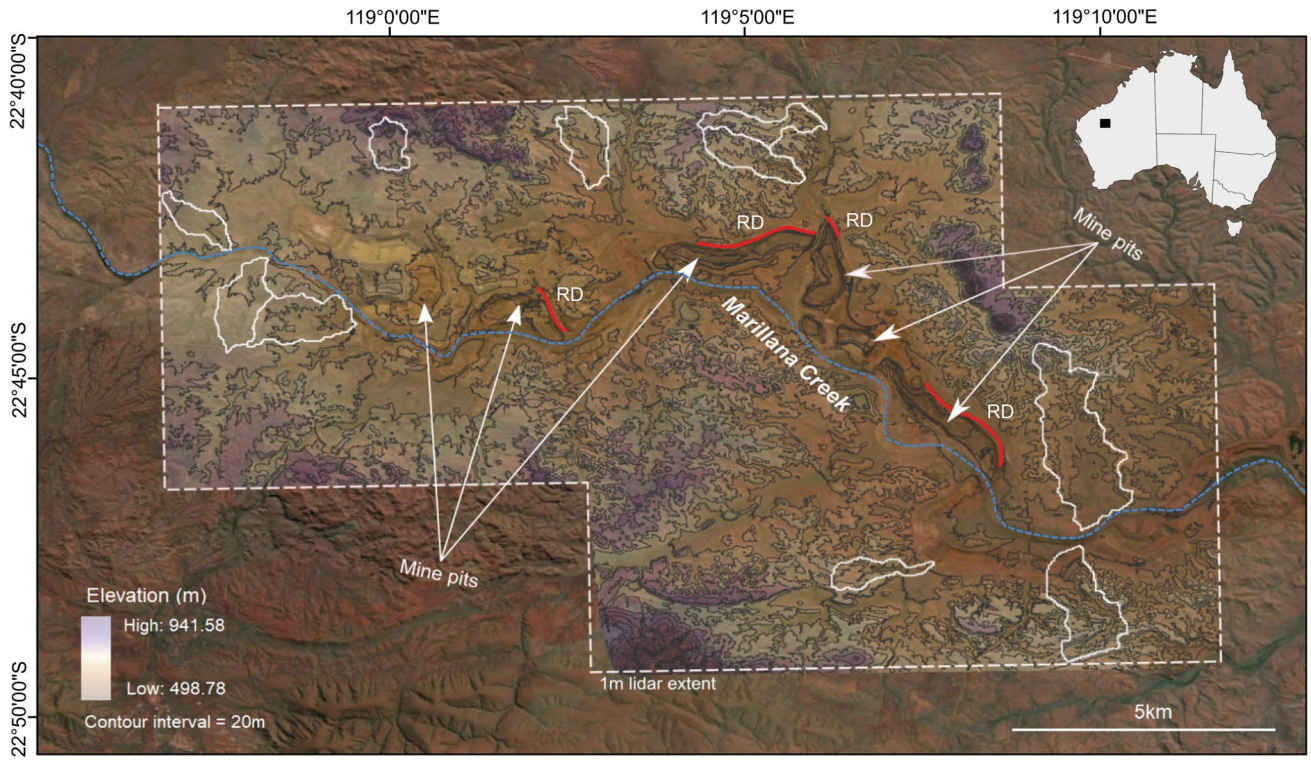

Fig. 3 Map of the Yandi mine site, in the Marillana sub-catchment, WA. Map shows the extent of the wide area map 1 m resolution DEM, with selected headwater catchments outlined in white. River diversion channels (RD) are shown in red

morphology with flow pathways either separated by inset transient bar formations or more stable island features.

Open-cut mine pits at the Yandi mine are over 80 m deep. RioTinto (2010) carried out simulations of the proposed post-mining landscape to estimate catchment hydrological conditions, assuming that headwater river diversion channels would be directed into the future pit voids. Their study found that 590 km^2 (26.5% of the total Marillana Creek system) would be truncated catchments if the diverted channels no longer flowed further downstream. The combined impact of the BHP and Rio Tinto mining operations within the Marillana Catchment was estimated to reduce channel flow by approximately 16.5% (BHP) and 10% (RioTinto), respectively, in addition to reducing river peak discharges by up to 46% at the Marillana Catchment outlet (Rio Tinto 2010).

Methods

General Approach

Natural headwater channels surrounding the Yandi mine site were investigated to describe their physical characteristics and derive hydraulic stability thresholds for the future design of river diversion channels. Ten headwater channels were split into a series of reach types previously described by Flatley et al. (2022). These reach types were used to classify natural channels upstream of the mine site, describe their variability, and produce reference sites as an example of the natural analogue of river diversion channels. Reference sites are largely unimpacted by anthropogenic activity and retain desirable natural characteristics (Blanchette and Lund 2017). This approach was selected due to the availability of appropriate reference reaches upstream of the mine site and because it is a standard approach used in river restoration and for the development of river diversion guidelines (State of Queensland 2019; White and Hardie 2000; White et al. 2014a; 2014b). Furthermore, each of the sites used in this investigation was previously surveyed by LiDAR, and a high-resolution 1 m digital elevation model (DEM) of the headwater catchments was available. A description of the headwater channels is provided in Table 1.

Using the natural headwater channels, we present a series of guideline values to quantify the typical hydraulic conditions found within each distinct reach type. To do this, a series of river flows of different size were modelled in the headwater channels using 2D hydrodynamic modelling (described below). Flow events in the reference reaches represented the 5-, 50-, and 100-year return interval (or the 0.2 average number of exceedances per year (EY), 2 and 1 annual exceedance probability (AEP)). Owing to a lack of stream gauges in these small channels, hydrological inputs

Table 1 Catchment description for natural channels used in this study

Catchment	Area (km^2)	Lat	Long	Equal area slope (m/km)	Channel length (km)
1	1.05	−22.712	118.956	18.54	1.13
2	0.96	−22.694	119.002	40.57	0.71
3	1.68	−22.695	119.046	16.65	1.10
4	1.48	−22.691	119.087	22.97	1.64
5	1.71	−22.697	119.085	37.61	1.55
6	1.95	−22.732	118.965	12.49	1.37
7	5.99	−22.766	119.159	22.48	2.06
8	3.23	−22.804	119.161	22.72	1.30
9	1.10	−22.796	119.109	26.71	1.17
10	2.42	−22.736	118.980	16.85	1.21

were quantified using a regional flood frequency estimation (RFFE) approach.

Cross sections provided at-a-station hydraulic geometry for each of the reach types within the headwater channels (Jowett 1998; Leopold and Maddock 1953; Singh and Zhang 2008). Model hydraulic output from flood simulations provided guideline hydraulic values (velocity, stream power (SP), and bed shear stress (BSS)) at each cross-section, which were spaced at 200 m intervals throughout the river reach types. Inherent variability within the river reaches was also considered by adopting the 25th-75th percentiles of hydraulic values for the development of closure criteria.

Modelling Channel Flows in TUFLOW HPC

Hydraulic values for the natural river channels were modelled using 2D hydrodynamic modelling using TUFLOW. TUFLOW HPC (heavily parallelised compute version) is a 2D fixed grid, adaptive time-step, hydrodynamic solver that uses an explicit finite volume solution (BMT 2018). TUFLOW HPC solves the full 2D shallow water equation, including a sub-grid eddy viscosity model. TUFLOW has shown good agreement with other 2D hydrodynamic software (Pasternack and Hopkins 2017). The scheme is both volume and momentum conserving, is 2nd order in space and 4th order in time, with adaptive or fixed time stepping, providing unconditional stability (BMT 2018). TUFLOW HPC was used to model these headwater channels due to the potential for significant changes in hydraulic conditions within the catchments. A flow-vs.-time (*QT*) boundary was used to apply a flow hydrograph directly to the 2D channel domain (Fig. 4), along with a water surface slope of 0.01 m/m. A grid size of 2 m was used to integrate detailed topographic forms such as smaller flowpaths and to capture the heterogeneity of the natural channels.

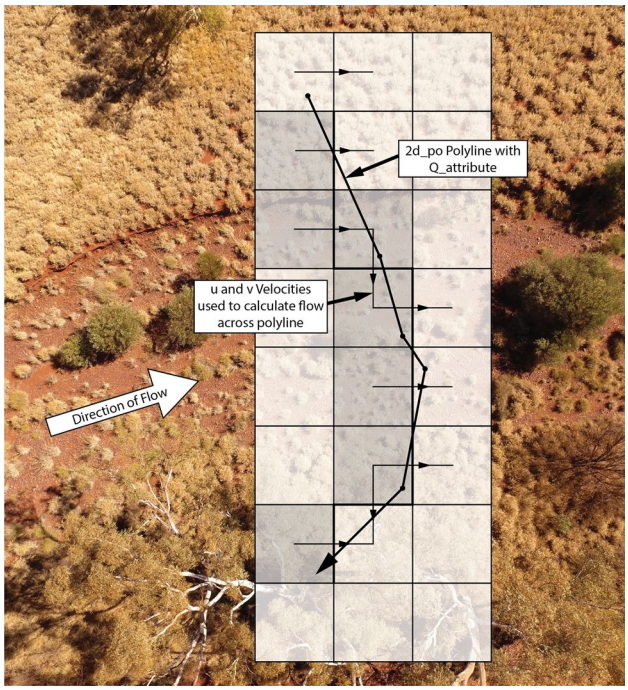

Fig. 4 Diagram showing a 2D Plot-output polyline (2D_po) and method of calculating flow across each cross section in the river channel. Each polyline is a digitised cross-section within the TUFLOW model of the river channels and a reporting location for hydraulic output (e.g. Q_attribute representing discharge). Modified from BMT (2018)

Hydrograph Creation

Hydrographs were created using a series of estimates derived to best represent peak discharge values for each annual exceedance probability. RFFE values are commonly used in ungauged catchments to estimate peak discharge (Rahman et al. 2012). Rainfall values were obtained from the Australian rainfall and runoff (ARR) intensity, frequency, duration (IFD) database. An index flood method (IFM; Davies and Yip 2014), a RFFE approach by Flavell (2012) and Australian Rainfall and Runoff (ARR) RFFE procedure (2015) were adopted to provide three sets of predicted peak discharge (Q_{peak}) values for the catchments. Flatley and Rutherfurd (2022) concluded that, in the Pilbara region, these approaches are best suited to estimating peak streamflow over other regionally derived RFFE (Table 2).

These estimated peak discharge values were used to create synthetic hydrographs across a range of return intervals. The time of concentration (t_c) equation was used to identify the time taken for the peak discharge to occur within each catchment to help design the rising limb of the synthetic hydrograph. The time of concentration equation used was an adapted Williams (1922) formula for ungauged catchments, as recommended by ARR1987:

Table 2 A description of how each of the RFFE methods calculates the flood peak

Method	Equation
ARR RFFE Model (2015 4th Edition)	$Q_x = Q_{10} \times GF_x$ with Q_{10} being: $\log_{10} = b_0 + b_1\log_{10}(\text{area}) + b_2\log_{10}(I_{6,50})$ where b_0, b_1 and b_2 are regression coefficients, estimated using OLS regression, area is the catchment area in km^2 and $I_{6,50}$ is the design rainfall intensity at catchment centroid for a 6-h duration and 50% AEP. The values of b_0, b_1 and b_2 and the regional Growth Factors (GF_x) are embedded into the RFFE Model 2015
IFM (Davies and Yip 2014)	For small catchment area (< 1000km^2) $Q_5 = 7.32 \times 10^{-8} A^{0.651} I_{1hr,2yrs}{}^{5.251}$ Frequency factors: 2ARI = 0.31, 5ARI = 1.0, 10 ARI = 1.70, 20ARI = 2.58, 50ARI = 4.15, 100ARI = 5.82
RFFP (Flavell 2012)	$Q_2 = 1.72 \times 10^{-64}\left(AS_e^{0.5}\right)^{0.8} LAT^{-12.17} LONG^{38.77}\left(\frac{L^2}{A}\right)^{-1.05}$ $Q_5 = 7.47 \times 10^{-46}\left(AS_e^{0.5}\right)^{0.81} LAT^{-14.62} LONG^{31.40}\left(\frac{L^2}{A}\right)^{-0.68}$ $Q_{10} = 2.36 \times 10^{-34}\left(AS_e^{0.5}\right)^{0.81} LAT^{-15.24} LONG^{26.28}\left(\frac{L^2}{A}\right)^{-0.39}$ $Q_{20} = 1.98 \times 10^{-23}\left(AS_e^{0.5}\right)^{0.79} LAT^{-15.08} LONG^{20.91}$ $Q_{20} = Q_{10}\frac{(13.21A^{0.61})}{(8.74A^{0.60})}$ With the largest value from each equation being adopted for the Q20: $Q_{50} = Q_{20} \times \text{frequencyfactor}\left(\frac{Q_{50}}{Q_{20}}\right)$ $Q_{100} = Q_{20} \times \text{frequencyfactor}\left(\frac{Q_{100}}{Q_{20}}\right)$ A = catchment area [km^2], S_e = equivalent uniform slope [m/km] and L = mainstream length [km]

$$t_c = \frac{58L}{A^{0.1} S_e^{0.2}} \quad (1)$$

where: t_c = time of concentration (mins), L = mainstream length measured to the catchment divide (km), A = Catchment area (km^2), and S_e = equal area slope of the mainstream projected to the catchment divide (m/km). The recession limb of the hydrograph was designed for a rainfall event of 12 h. This duration was selected to represent the infrequent, yet heavy rainfall from seasonal thunderstorms, tropical low-pressure systems, and cyclonic events (Aryal et al. 2020). Additionally, this timeframe was long enough to capture the peak discharge across all headwater catchments. The synthetic hydrographs were then applied

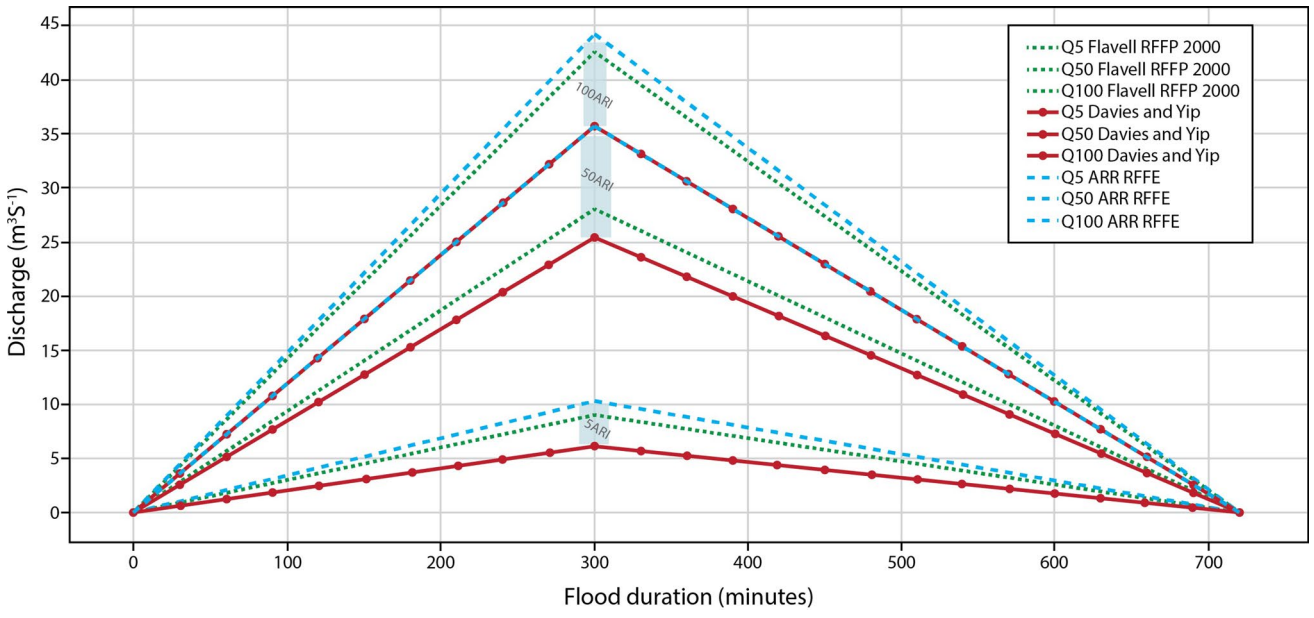

Fig. 5 Example of synthetic hydrograph used in modelling of flood flow events within natural headwater channels. Hydrograph shows Flavell RFFP (2000), Davies and Yip (2014), and ARR RFFE (2015) approaches

as the flow-vs.-time (QT) boundary into the 2D domain in TUFLOW to create the flood flows within the river channels. Figure 5 provides an example of hydrographs used for the flood modelling where the peak was calculated using this approach.

Channel Characterisation

Channel reaches featured distinct geomorphic units and variable substrates, which have a large influence on the underlying roughness conditions within the catchment. Flatley et al. (2022) provide guideline Manning's n values for each headwater channel type in the Pilbara region through a high-resolution analysis of channel form. Confinement was defined as the percentage of the length of a stream or river channel segment that abuts a confining margin on either bank (Fryirs et al. 2016), and considered through visual assessment of the confining margins within each reach to derive confined, semi-confined, and unconfined reaches. Channels were then classified as single channel, or multithread. In this instance, multithread was used to describe a channel separated by alluvial in-channel islands that are either well-formed and vegetated or nascent and emerging. Single channels were further divided by bed material as sand, cobbles, or bedrock. Where the channel cross section was highly vegetated and

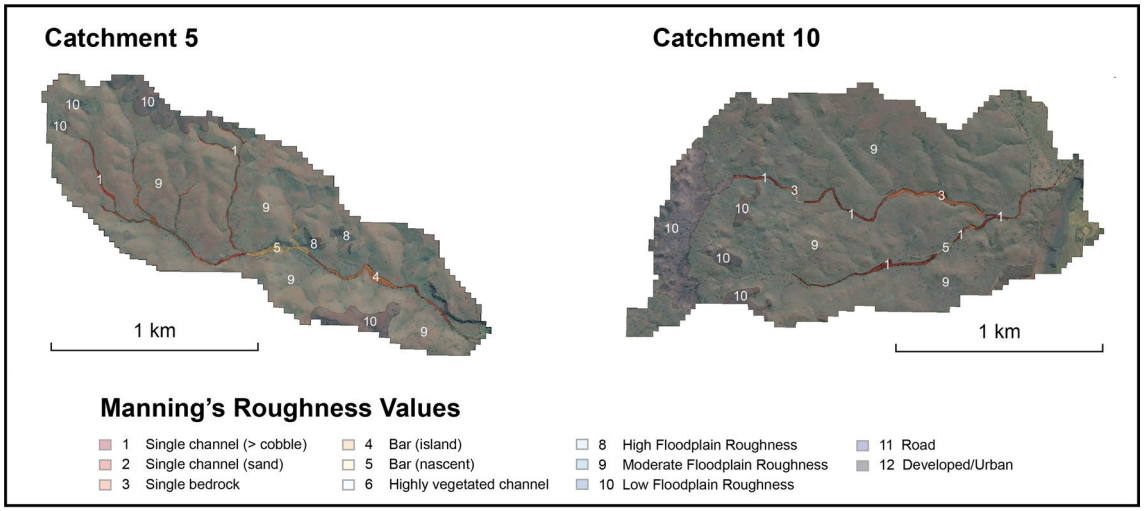

Fig. 6 Example of Manning's roughness values assigned in the TUFLOW materials file for catchment modelling. Each reach was assigned a unique Manning's class. Further information on reach descriptions can be found in Table 3

Table 3 Manning's roughness (n) values derived from Limerinos (1970) for headwater channels (from Flatley et al. 2022) and floodplain units within the hydrodynamic model

Class	Channel or floodplain type	Description	Manning's n
1	Single channel (≥ cobble)	Single-thread channel with cobble sized D_{50} fraction (or larger)	0.0427
2	Single channel (sand)	Single-thread alluvial channel with sand-sized D_{50} fraction	0.0274
3	Single bedrock	Single mostly bedrock channel	0.055
4	Bar (island)	Alluvial channel with vegetated islands	0.047
5	Bar (nascent)	Single-thread channel with small vegetated nascent barforms covering the channel	0.046
6	Multithread	Multithread channel with cobble-sized sediment	0.038
7	Highly vegetated channel	Highly vegetated channel where the channel boundary cannot be discriminated	0.07
8	High floodplain	Highly vegetated floodplain or irregular topography	0.035
9	Moderate floodplain	Sandplain, lightly vegetated desert soils	0.03
10	Low floodplain	Mesa, cliff-face, bedrock, uniform desert pavement	0.025
11	Road	Dirt roads	0.016
12	Developed/Urban	Paved roads and mining infrastructure, including rail networks	0.022

Manning's classes 8–12 assigned using the Modified Cowan Method (Cowan 1956)

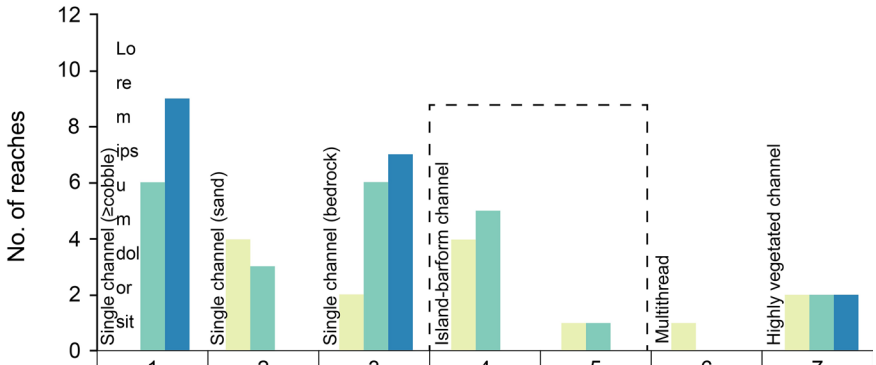

	1	2	3	4	5	6	7
No. Unconfined	11	4	2	4	1	1	2
Semi-Confined	6	3	6	5	1	0	2
Confined	9	0	7	0	0	0	2

Fig. 7 Channel reach types used for developing design guidelines. Figure shows the variety of reach types within the modelled catchments surrounding the mine site

no planform was able to be determined, river reaches were classified as a heavily vegetated channel.

To quantify the diversity in channel types, a digitised vector-based materials layer was added to the TUFLOW model that had the associated roughness parameter (Manning's n) for each channel type. Wider floodplain roughness values were also adopted using the modified Cowan method (Cowan 1956) where floodplain values were categorised into high (n = 0.035), moderate (n = 0.03), and low (n = 0.025) floodplain roughness values (Fig. 6 and Table 3).

Model Output

TUFLOW simulations were set up to map the flood output for flows of different recurrence interval. Model outputs were maps of bed shear stress (*BSS*), specific stream power (*SSP*), and velocity (*V*), which were used to create hydraulic reference criteria, in addition to water depth (*d*), and Courant stability (a measure of model stability). Stream power (Ω) is calculated in TUFLOW using the following:

$$\Omega = |V|\tau_{bed} \tag{2}$$

The default cut-off depth for BSS and SP calculations in TUFLOW is 0.1; at depths less than this, the map output data will linearly reduce to zero (BMT 2018) because the BSS formula divides by the water depth. From the stream power (Ω) output, specific stream power was derived:

$$\omega = (pgQS)/w \tag{3}$$

where Q is the discharge (in $m^3\ s^{-1}$), w is the width of the water surface (in m), S is the longitudinal slope (in m/m^{-1}), ρ is the fluid density (in kg m^{-3}), and g is the acceleration due to gravity (in m s^{-2}).

Critical bed shear stress thresholds for each sediment sample size were determined using the thresholds from Julien (1998) provided in supplemental Table S-1. Sediment mobility occurs when the bed shear stress (BSS) exceeds the critical shear stress for a given particle size. Sediment transport was mapped within the modelled river channels using the output BSS to help quantify sediment transport at different flood return intervals.

The average of the values obtained from each of the RFFE methods was used to derive the guideline hydraulic criteria for each channel type. For the creation of guideline hydraulic criteria, the 25th and 75th percentile of velocity, SSP, and BSS values were applied from each reach type. This was to address the variability within each river reach, to establish the reference hydraulic conditions within the channel types, and to follow similar methodology for the development of other river diversion guidelines within Australia (White and Hardie 2000; White et al. 2014a; 2014b).

Results

We first present the variety of headwater channel types within the modelled river reaches. Overall, velocity, SSP, and BSS values were obtained for 66 cross sections across 10 modelled catchments. Seven distinct channel types were identified within confined (27.3% of reaches), semi-confined (34.9% of reaches), and unconfined (37.9% of reaches) geomorphic settings. The inventory of reach types were: single channel (≥ cobble) n = 26, single channel (sand) n = 7, bedrock n = 15, island-barform n = 11, multithread n = 1, and highly vegetated channel n = 6 (Fig. 7). Peak hydraulic parameters (velocity, SSP, and BSS) estimated at each cross-section from the TUFLOW model output are presented below.

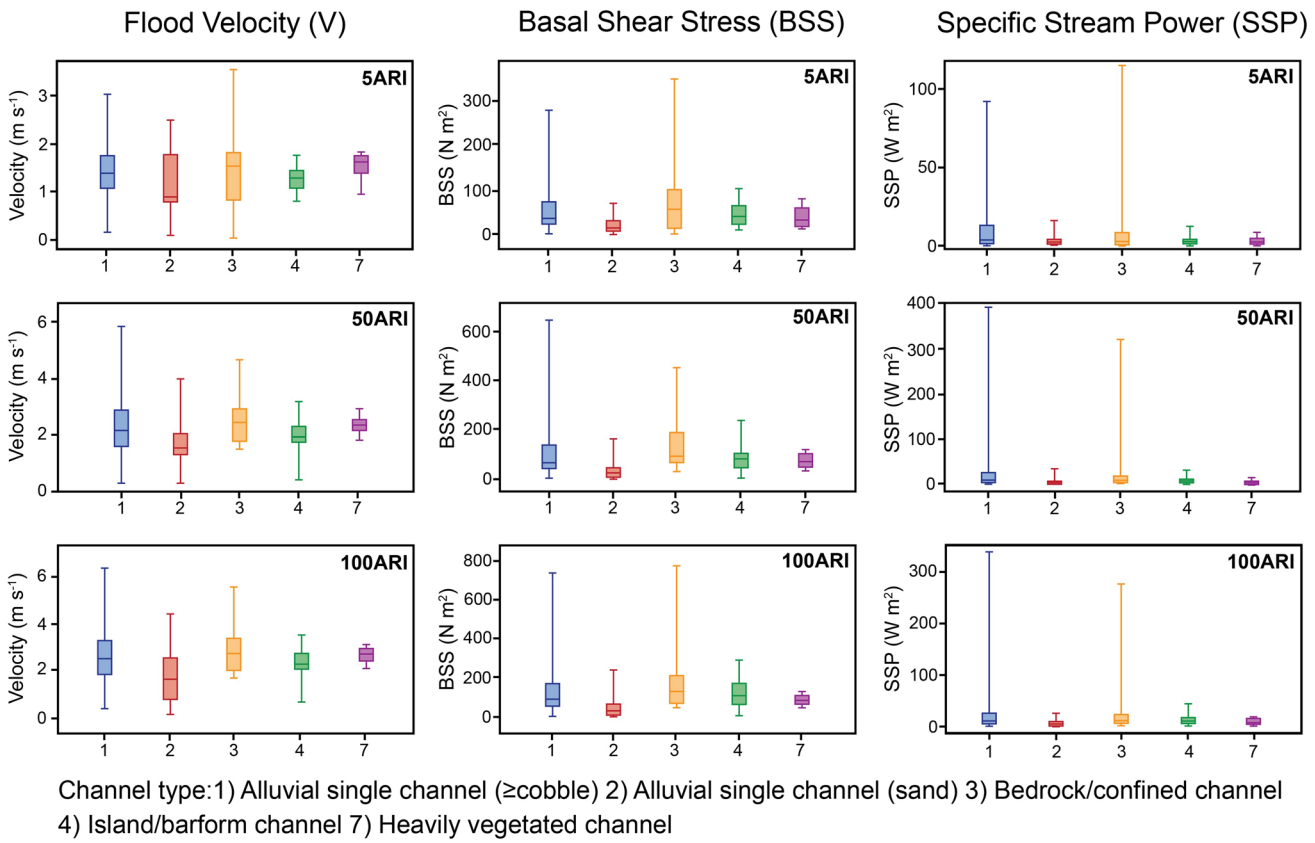

Fig. 8 Box and Whisker plots showing average hydraulic results for the different channel types produced from mean values of each streamflow estimation method. The flood velocity, bed shear stress, and stream power for each reach type are shown for the 5, 50, and 100 year ARI

Natural Channel Hydrogeomorphic Conditions

Figure 8 shows average hydraulic values across each channel type. These averages were derived by taking the mean hydraulic values from each flow event using the Flavell RFFE 2000, IFM, and ARR RFFE approaches for 5, 50, and 100 year return interval flows. The hydraulic outputs of each of these methods can be found in supplemental Tables S-2, S-3, and S-4.

There are some key observations from the simulations and derived average hydraulic values. Firstly, there are consistent average hydraulic values (velocity, BSS, and SSP) across reach types for all of the simulated ARIs, with more variation in the 25th-75th percentile values between reach types. Bedrock sections have higher mean velocities, BSS, and SSP. However, there is a greater range in the hydraulic parameters for single channel (≥ cobble) reaches. The BSS and SSP is lowest in alluvial sand channel, island-barform, and heavily vegetated channels. The range of BSS and SSP are low for heavily vegetated channels, but this channel type was only represented by six cross sections. There is only a small increase in values for velocity, SSP, and BSS between the 50 ARI and 100 ARI flows.

Table 4 shows derived hydraulic guidelines for all channel types for a 5, 50, and 100 ARI flood. These hydraulic guidelines represent the 25th-75th percentiles of values from peak discharges at each cross section. Even when using this range of values from the reach types, there is only a small increase in the 75th percentile values as the flood magnitude increases.

These values represent the peak of flood conditions within the channels. These guidelines were simplified and are provided in Table 5. The interpretation of these observations follows in the discussion.

Sediment Transport Thresholds

This section describes the thresholds for sediment transport in the modelled reaches. As an example, Fig. 9 shows the flood modelled scenarios for Catchment 1 across the 5, 50, and 100 year ARI flows. The figure also shows the areas of the bed where the BSS exceeds the threshold for transporting specific grain sizes of bed material. The flow

Table 4 Range of average hydraulic values derived from all flood estimation methods

Channel type	5 ARI	50 ARI	100 ARI
Velocity (m/s)			
All headwater channels combined	0.9–1.7	1.6–2.6	1.9–3
Single channel (≥ cobble)	1.1–1.7	1.6–2.8	1.8–3.3
Single channel (sand)	0.8–1.6	1.4–1.8	0.4–2.1
Bedrock/confined channel	0.9–1.8	1.8–2.9	2.1–3.3
Island barform channel	1.2–1.4	1.8–2.2	2.1–2.6
Heavily vegetated channel	1.5–1.7	2.2–2.5	2.5–2.8
Stream power (W/m^2)			
All headwater channels combined	0.7–5.5	1.7–14.79	2.7–14.5
Single channel (≥ cobble)	1.3–12.6	1.7–22.29	2.7–22.2
Single channel (sand)	0.5–2.4	0.5–2.34	1.6–7.2
Bedrock/confined channel	1.3–8.1	2.9–14.50	5.2–17.7
Island barform channel	1.3–2.9	2.9–7.23	5.9–14.1
Heavily vegetated channel	1.5–3.1	2.6–6.31	4.2–11.5
Bed shear stress (N/m^2)			
All headwater channels combined	15.8–72.2	43.2–120.3	50.9–164.0
Single Channel (≥ cobble)	25.4–69.5	44.0–135.0	54.1–156.1
Single channel (sand)	9.4–22.8	11.1–37.5	13.6–51.3
Bedrock/confined channel	14.9–95.7	70.0–169.4	73.4–200.3
Island barform channel	24.4–60.1	52.8–100.6	65.8–155.5
Heavily vegetated channel	19.7–51.9	50.6–93.1	63.4–102.8

pathways adjust from a single channel to a multithread channel as flood magnitudes increase. The flood modelling demonstrates that the 50 year ARI flood occupies most of the floodplain, and that the 50 and 100 year ARI floods produce much higher BSS within the channel bed and banks than does the 5 year ARI flood. It also shows that highest shear stresses are concentrated in confined channel sections.

Figure 10 shows the same flow bifurcation in catchment C2. In this instance, the overbank flow coincides with the location of a minor tributary junction where the incoming flow was not included as part of these models. This bifurcation of flow likely causes backwater flow conditions at the junction in addition to greater submergence of flow within the floodplain. At greater flow conditions (50 and 100 year ARI), the floodplain area around this bifurcation is submerged. Additional backwater flows occur at the downstream tributary junction south-east of the mining camp. Maximum critical BSS values indicate that coarse gravel sediments (with a BSS of 12.2 N/m^2 or higher) are readily mobilised in local settings at the peak of a 5-year ARI flood. During the 50 and 100 year ARI events, there is substantial mobilisation of very coarse gravels to coarse cobbles (BSS = 12.2 to 112 + N/m^2). During these floods, it is likely that boulders will also be transported in high BSS areas within these headwater channel settings. Additionally, Fig. 11 shows the critical BSS for Catchment 7 and the inundation of the floodplain within a semi-confined setting. The mapped output indicates that low floodplain inundation occurs at the 5 year ARI flow events, with greater bifurcation occurring at the 50 and 100 year ARI.

Figure 12 shows Catchment 9, highlighting that flood flows remain within the confined channel. Within this channel, all floods produce peak critical BSS values capable of moving larger sediments (coarse gravels and higher). This shows that in this headwater channel, floods can mobilise sediments effectively within the upstream section of the catchment (left side of the figures) before a drop in BSS toward the channel's catchment outlet.

Discussion

Similarity of Average Hydraulic Conditions

This paper provides hydraulic characteristics of 10 headwater channels in the Pilbara, for the estimated 5, 50, and 100 year ARI floods. These characteristics can provide guideline values for designing small mining diversions. The results indicate the surprisingly uniform mean hydraulic values (*of velocity, BSS, and SSP),* as indicated by the box and whisker plots differentiated by channel type (Fig. 8). A study of ephemeral headwater channels in the Sonoran Desert also found that piedmont headwater, bedrock with alluvium, and

Table 5 Proposed guideline hydraulic values for natural headwater channels

Stream Type	Velocity (m/s)			Stream power (W/m^2)			Bed shear stress (N/m^2)		
	5 ARI	50 ARI	100 ARI	5 ARI	50 ARI	100 ARI	5 ARI	50 ARI	100 ARI
All headwater channels combined	1–2	2–3	2–3	1–6	5–16	6–26	16–72	48–124	50–164
Single Channel (≥ cobble)	1–1.7	1.6–2.8	1.8–3.3	1.3–12.6	1.7–22.3	2.7–22.1	25.4–69.4	44–135	54–157
Single channel (sand)	0.8–1.6	1.35–1.8	0.4–2.0	0.4–2.3	0.2–1.9	0.8–6.4	9.4–22.8	11–38	14–51
Bedrock/confined channel	0.9–1.8	1.8–2.9	2–3.3	0.9–8	2.9–14.5	5.1–18	14.9–95.7	70–170	73–200
Island barform channel	1–1.4	1.8–2.2	2–2.5	1.3–2.9	2.9–7.2	4.3–14	24.4–60	52.8–100	50–144
Heavily vegetated channel	1.5–1.7	2.2–2.5	2.5–2.8	1.5–3.1	2.6–6.3	4.2–12	19.7–51.9	63–103	44.95–55.76

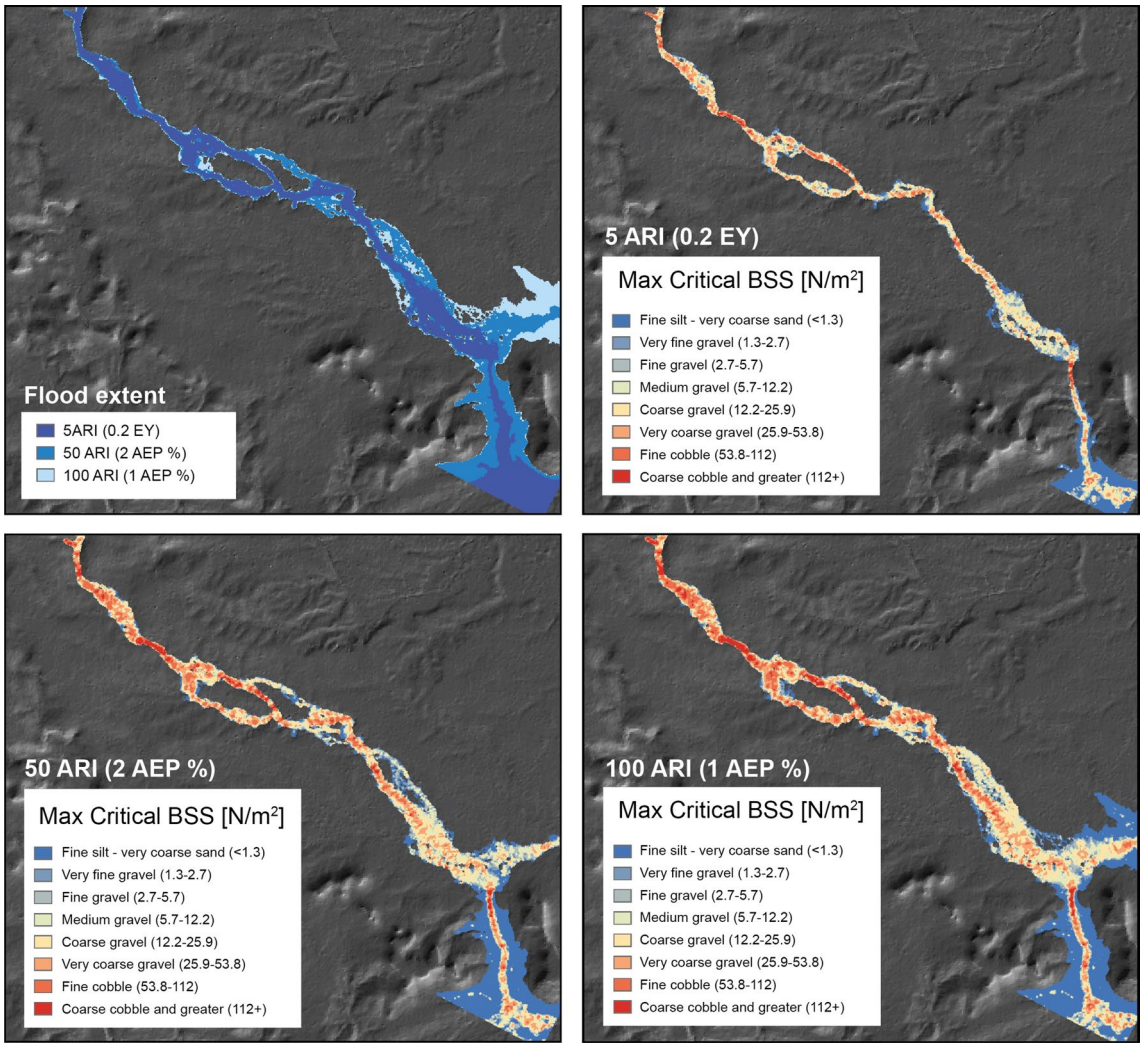

Fig. 9 Flood extent and critical bed shear stress for C1 across the 0.2 EY, 2 AEP (%), and the 1 AEP (%). Flood extent has been clipped to show the catchment outlet

braided river channels had similar mean unit stream power (W/m^2) and mean dimensionless shear stress for a similar reference water level (Sutfin et al. 2014). A potential explanation for the similarity of shear stress for differently sized floods is the interaction between in-channel roughness and floodplain resistance. When the flow occupies the channel in the 5 year ARI flood, roughness is provided by elements within the channel. As flow moves onto the floodplain, the resistance is provided by the shallow depth of flows across the floodplain. Local areas of overbank flow in low flow events also moderate shear stress, identified elsewhere as an adjustment of channels to equilibrium conditions and a machanism for channels to remain stable dispite large floods (Tooth and Nanson 1999).

However, longitudinal variability in the river channels (e.g. moving from a cobble to sand substrate) also helps control the overall hydraulic conditions. During large floods (50–100 year ARI), when flood flows reach unconfined sections, flows exit the channel and move overbank onto the surrounding alluvial plain. Mean velocities in sections with greater overbank flood flows (e.g. sand channels) tend to decline as the surrounding floodplain is inundated. This reduction in velocity is also observed in larger dryland channels. Maximum velocity has been shown to continue to increase beyond bankfull in anastomosing river channels in Channel Country, Australia (Knighton and Nanson 2002). However, velocities decline once the relative floodplain depth reaches 0.2–0.25 m, a depth identified at which channel-floodplain interactions are likely to be at a maximum (Knight and Shiono 1996) and the shallower floodplain flow significantly slows the main channel flow (Knighton and Nanson 2002). The same

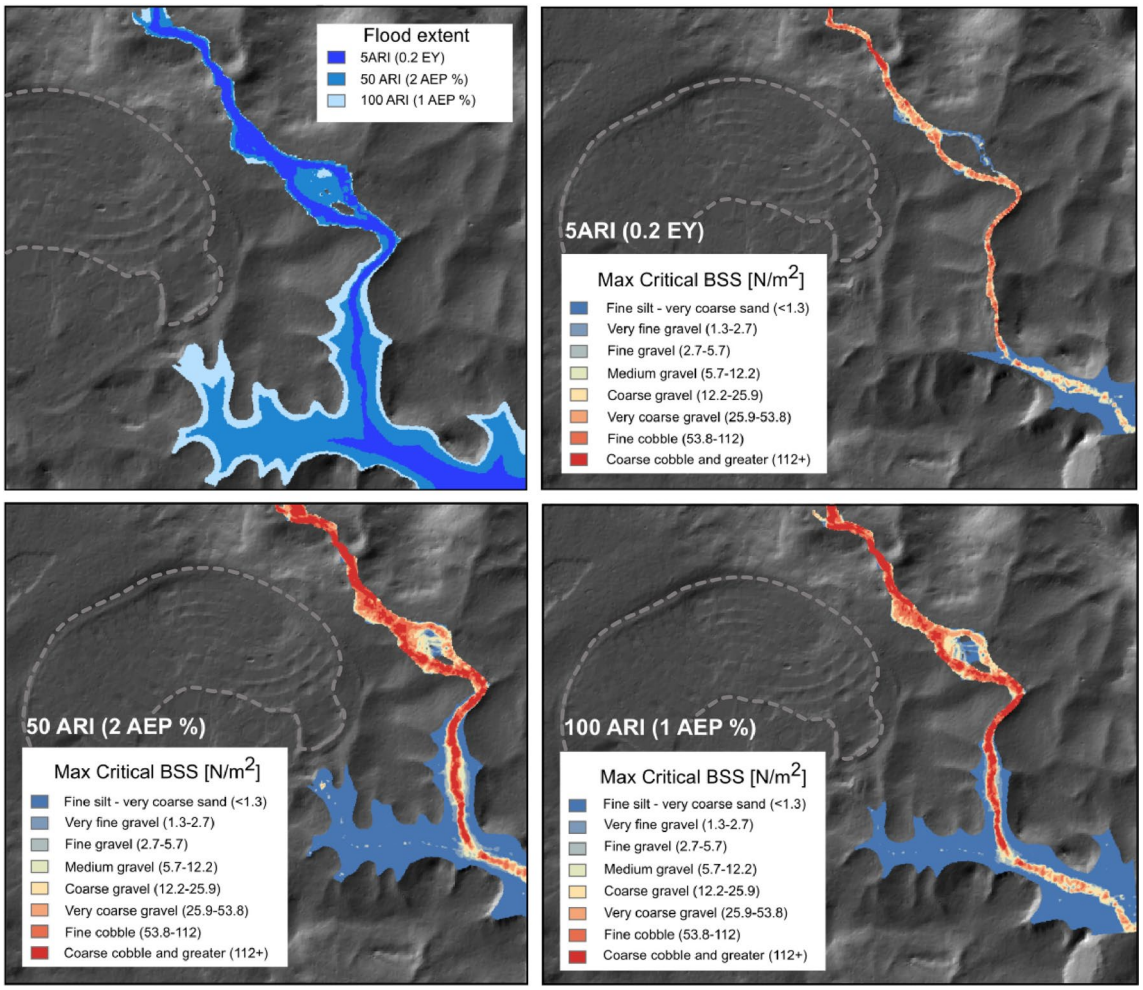

Fig. 10 Flood extent and critical bed shear stress for C2 across the 0.2 EY, 2 AEP (%), and the 1 AEP (%). Dashed line shows the extent of a mining camp. The flood extent has been clipped to show the catchment outlet

effect is seen here in the modelled headwater catchments between single channel (≥ cobble) and single channel sand reaches. Although there is an increase in hydraulic values between the 50 and 100 year ARI, it is likely that heightened overbank flows is a key control for the overall small change in hydraulic values.

Additionally, barform reaches within our study exhibited similar hydraulic conditions across the 50 and 100 year ARI. As flows diverge around the barform, flow is dissipated and the flood is unable to transport larger materials (coarse cobbles and larger) in the newly activated part of the channel (e.g. Figure 10). These barforms are unlikely to be completely restructured by flood disturbances and their form initiates feedback loops of increased roughness, vegetation establishment, and finer material deposition. They remain resilient to disturbances through natural processes (Sutfin et al. 2014) and help moderate velocities, BSS and SP within the channel by providing greater hydraulic roughness.

Importance of overbank flow in headwaters

The hydrogeomorphic modelling undertaken here displays the importance of the floodplains in headwater channels, even within small, high-slope catchments. It is difficult to fully mimic headwater channels without including the floodplain in the final landform design. During mine operation, river diversions most resemble confined bedrock channels without a floodplain. However, in most instances, the headwater channels also have unconfined sections, where the floodplain helps dissipate energy within larger river flow conditions, helping to minimise excessive erosion within the channel. Therefore, to maintain natural sediment transport rates within the channel, overbank flooding is required. If the diversion channel does not have a floodplain channel, flow will transport larger sediments and have greater energy, prompting in-channel erosion through bank collapse and heightened headcutting within the channel.

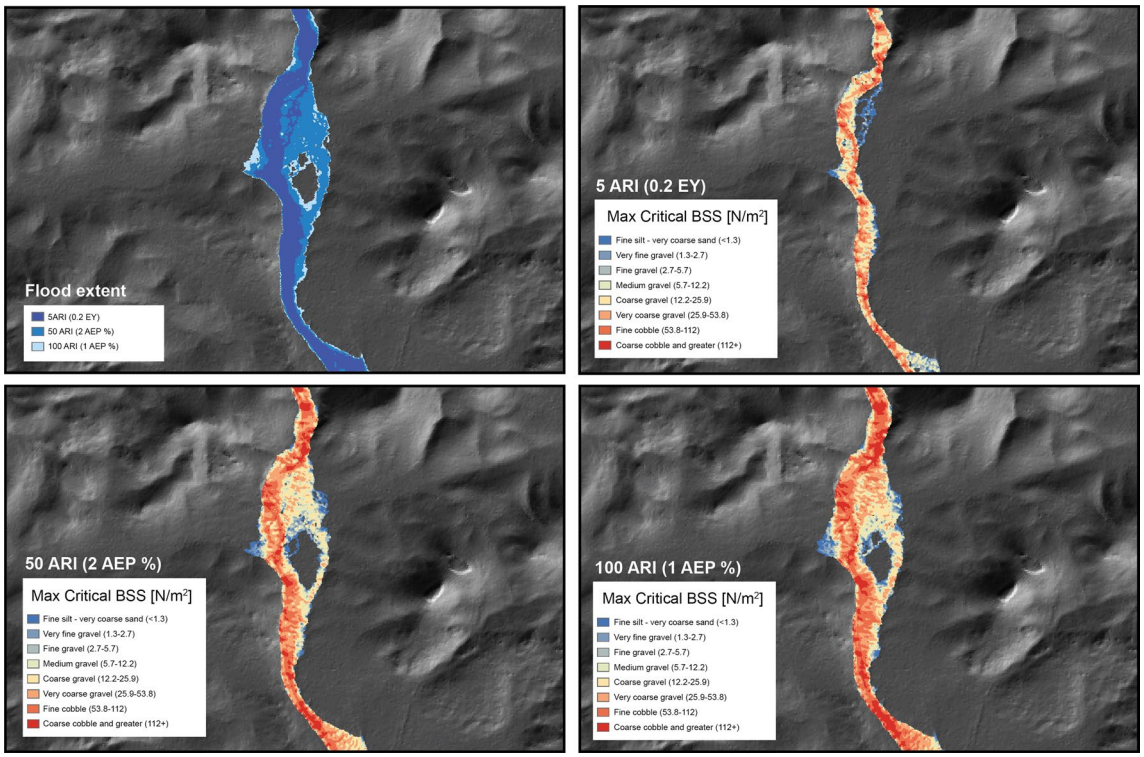

Fig. 11 Flood extent and critical bed shear stress for C7 across the 0.2 EY, 2 AEP (%), and the 1 AEP (%). Flood extent has been clipped to show the catchment outlet

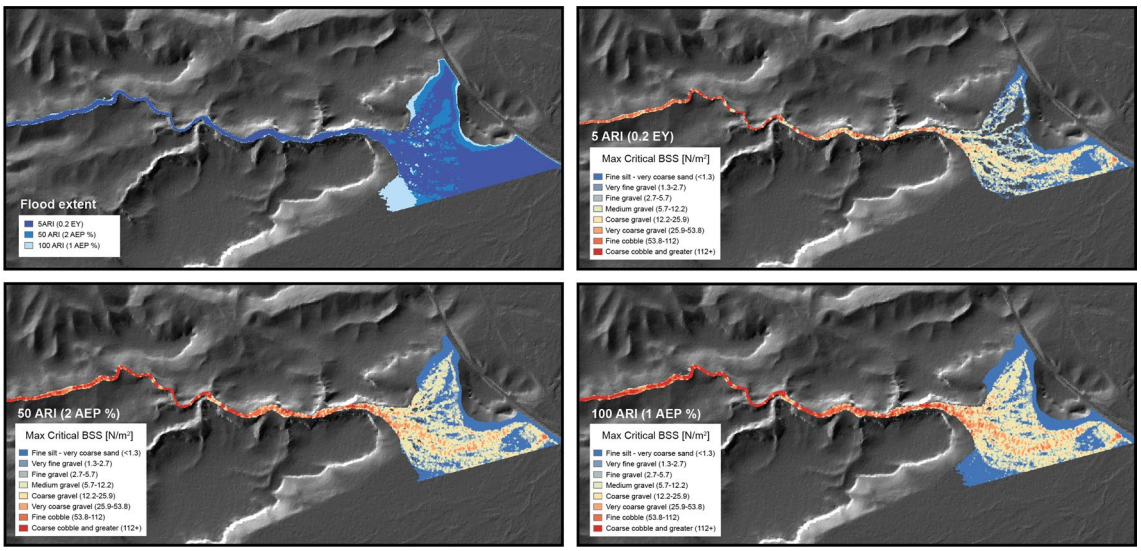

Fig. 12 Flood extent and critical bed shear stress for C9 across the 0.2 EY, 2 AEP (%), and the 1 AEP (%). Flood extent has been clipped to show the catchment outlet

Additionally, local overbank floodplain flows are also important in more frequent floods (e.g. 5 year ARI). Even in frequent floods, channel flows spill over banks to form localised multithread sections. Modelling the flood flows has enabled the visualisation of the flowpaths of the river network and determine areas where this lateral overbank flow occurs, which would be challenging to observe or interpret based on channel form alone. Flow events of 50 year

ARI and above often leave the defined channel, causing a diffusive flood flow across the floodplain toward the bottom of the defined catchment, with strong lateral connectivity to the floodplain.

Channel boundary variability in addition to hydrologic variability was identified by Brown and Pasternack (2014) as creating hydrodynamic spatial patterns in headwater rivers through process-blending, determining spatial structure and sediment dynamics. In this study, hydrodynamic modelling suggests that a variety of specific channel geomorphic responses occur across different flow regimes to control hydraulic conditions within the channel, making the overall mean hydraulic values supriusingly uniform.

Modelling Geomorphic Work

The hydrodynamic modelling output and the sediment transport thresholds also help inform the geomorphic work carried out at different flow magnitudes helping to visualise small-scale channel aggradation (e.g. the pulsing of finer sediment and creation of small nascent bar forms) during the 5 year ARI, in addition to the proportion of the floodplain occupied at different sized floods.

The presence of backwater flow was identified at tributary junctions across all flood magnitudes above 5 year ARI, which leads to increased flood water levels in backwater sections. Additionally, the headwater streams have alternating sections of high velocity, low depth, and high depth, low velocity, with features analogous to the pool-riffle sequence in perennial streams. The 'riffle' in these headwater channels is produced by four major features; backwater flow features at tributary junctions, stable channel islands, incipient nascent migrating bar forms, and localised obstructions formed from debris dams and submerged vegetation from trees and larger riparian plants. Variable bank heights in the channel create localised sections across the river's longitudinal profile where the bank height is lower than the opposing bank, allowing for channel flow to easily dissipate across the floodplain (as described above).

High-Energy, Highly Erosion-Resistant Surfaces

Across the modelled channel networks, there were areas of local high SSP and BSS values, indicating that coarse sediments will be mobilised and transported during small floods. Overall, the reach types displayed high BSS values at a 5 year ARI. The exception to this was in sand reaches, where the BSS sits between 9–23 N/m^2 (Table 5), which indicates mobility of coarse gravel within these reaches even at a 5 year ARI.

However, the critical shear stress values used in the model can be further refined for headwater channel sediments found within the Pilbara region due to the high proportion of denser iron-rich sediments. Many of the sediments in the vicinity of the mine are derived from the erosion of banded iron formation (BIF), resulting in a high proportion of iron-rich sediments, with a density of 2.85–3.15 g/cm^3 (James 1966), compared to quartz (2.65 g/cm^3). The bulk density of rocks within the Hamersley province can vary between unaltered BIF with an average bulk density of 3.24 g/cm^3 to high grade hematite with a density of 4.30 g/cm^3 (Webb 2003). Secondary iron ores such as CID and detrital iron deposits are found extensively in the area (Morris 2015) and these are coarse colluvial gravels that largely retain the characteristics of the BIF or variably ferruginised surface BIF from which they are derived (Kneeshaw and Morris 2014). As a result, iron-rich sediments have a higher particle density resulting in a more erosion resistant substrate in the river channels. Additionally, secondary armouring of iron-rich sediments also occurs through the formation of ferricrete and canga cover (Gagen et al. 2019; Levett et al. 2019), which can form a superficial cover over erosion surfaces (Kneeshaw and Morris 2014).

Within our model, we calculated the sediment transport thresholds with critical BSS thresholds for quartz-dominant sediments as BIF alternates between iron-rich and quartz-rich bands. However, our thresholds therefore represent thresholds for quartz-dominant sediments within the channel. The presence of denser iron-rich sediments has consequences for sediment transport and armouring within the channel as denser particles require higher BSS to mobilise them during floods, and patches of canga cover can create localised armouring on the surface. Additionally, vegetation plays a key role in the erosive resistance of the channel, creating channel hydraulic resistance during flow events and subsequently stabilising sediments within the channel. A combination of these factors may mean less sediment is ultimately mobile at each ARI.

Field observations show that plant-associated precipitation of iron oxides may occur, with plant-driven cementation of canga fragments being observed around the base of plants in other BIF areas (Gagen et al. 2019). Ferricrete under shrub heath within Western Australia has also displayed Fe-lined root channels, which was concluded to be evidence of the role that plants play in niche-building processes (Verboom and Pate 2006). Therefore, the role of iron-rich lithology, regolith, and plant establishment is complex, and undoubtedly a key control on the geomorphic stability of these headwater channels.

Derivation of Reference Criteria (Design Guidelines)

The use of 2D hydrodynamic modelling allows for the representation of the physical processes and flow conditions that would otherwise be challenging to observe or interpret based on channel form alone. Alongside the creation

of guideline hydraulic reference criteria, interpreting flow events within headwater channels offers an opportunity to learn more about flood dynamics in a setting where flow events are highly sporadic and largely ungauged. Creating distinct channel types and incorporating variable roughness into the flood models allowed for the simulation of realistic flood events for each catchment, helping one to identify the variability and variety of these headwater channels.

The developed reference criteria act as a benchmark for understanding natural channel conditions and can help engineers and managers design a permanent river diversion that best replicates hydraulic conditions found within local headwater channels by understanding reference reach conditions. These guidelines provide a template for distinct reach types and highlight the importance of localized longitudinal fluctuations in velocity, SSP, and BSS in headwater channels. Headwater channels in the Pilbara display a diverse array of geomorphic components that are spatially distributed along the stream profile and help dissipate river flood energy, particularly within larger flood flows (50–100 ARI). However, establishing in-channel features such as nascent bars, islands, and vegetation can also contribute toward the local longitudinal variability of hydraulic values and create channel boundary variability, encouraging localised overbank flow at 5 year ARI.

We can compare the hydraulic reference criteria developed in this paper with ACARP criteria (White et al. 2014b) by assessing differences across flow frequencies for the different channel types (Table 6). Headwater streams in our study best align with the ACARP bedrock controlled and supply limited stream types; however, localised reaches have greater sediment supply. The stream power within the headwater channels of our study is significantly less than the ACARP guidelines across both rare and frequent flood flows whereas the velocity values show some similarity. The difference is because the channels here were often smaller and more confined than the ACARP channels, with the narrow widths causing a surge of velocity compared to a much larger channel with a higher overall discharge spread over a wider channel extent.

Overall, the BSS values within our study exceeded the ACARP guidelines across the 5 year ARI frequent floods, with the exception of the sand bed single channels modelled in this study that had a 25th-75th percentile of 9.4–22.8 N/m^2 for a frequent flood flow and 11–38 N/m^2 for a rare flow. Therefore, if you were to construct diversions based on ACARP in the Pilbara, it is not likely you would be able to recreate the sandy reaches observed in this setting. Additionally, the other channel types show a much higher shear stress in the frequent flooding events compared to ACARP guidelines. If using the ACARP guidelines to construct diversion channels in the Pilbara, it is likely that the river diversions would be constructed larger to redistribute these projected higher bed shear stresses into a wider and deeper channel. Therefore, the ACARP guidelines do not fit well with the headwater streams modelled here, and they do not match the observed variations in SSP, velocity, and BSS across the varied reach types found in our study. Overall, these results show that the existing ACARP criteria for river diversions (commonly used in Queensland but sometimes applied in Western

Table 6 Comparison of the hydraulic values derived in the headwater channels in the Pilbara compared with the ACARP criteria (Queensland) where ACARP values are derived from White et al. (2014b)

Stream type	Velocity (m/s)		Stream power (W/m^2)		Shear Stress (N/m^2)	
	Frequent floods (2ARI-5 ARI)	Rare (50 ARI)	Frequent floods† (2ARI-5 ARI)	Rare Floods (50 ARI)	Frequent floods (2ARI-5 ARI)	Rare floods (50 ARI)
This study						
All headwater channels	1–2	2–3	1–6	5–16	16–72	48–124
Single channel (≥ cobble)	1–1.7	1.6–2.8	1.3–12.6	1.7–22.3	25.4–69.4	44–135
Single channel (sand)	0.8–1.6	1.35–1.8	0.4–2.3	0.2–1.9	9.4–22.8	11–38
Bedrock/confined channel	0.9–1.8	1.8–2.9	0.9–8	2.9–14.5	14.9–95.7	70–170
Island barform channel	1–1.4	1.8–2.2	1.3–2.9	2.9–7.2	24.4–60	52.8–100
Heavily vegetated channel	1.5–1.7	2.2–2.5	1.5–3.1	2.6–6.3	19.7–51.9	63–103
ACARP						
Supply limited (low sediment supply)	1–1.5	1.5–2.5	15–35	50–100	< 40	< 100
Transport limited (high sediment supply)	0.5–1.1	0.9–1.5	35–60	80–150	< 40	< 50
Bedrock controlled	1.3–1.8	2.3	50–100	100–350	< 55	< 120

The hydraulic values in this study were created for a 5 year ARI whereas the ACARP values are for a 2 year ARI, but these both fall under the frequent flood range and are therefore compared as such

†Frequency descriptor comes from the Australian Rainfall and Runoff (ARR2016) preferred terminology for flood risk (Book 1, Chapter 2.2.5)

Australia) are not appropriate for the long-term design of small headwater channels, requiring a new industry standard for these types of river diversion in the Pilbara region.

Applicability and Limitations of the Hydraulic Guideline Criteria

The hydraulic values presented here can be used to help create new reference criteria to drive the design of a final river diversion channel in the Pilbara and to create a final landform that is stable, with room for geomorphic processes to occur within their natural range. Additionally, they can be used as a benchmark for existing river diversion channels that may not be performing adequately. These guidelines are suitable for smaller catchments (e.g. < 10 km^2) and should be used with care in catchments larger than the reference reaches modelled here. Overall, an improved understanding of the hydraulic conditions required for the deposition and accumulation of finer sediments within a river diversion channel can help engineers create the right conditions to encourage geomorphic feedbacks with vegetation establishment and continued geomorphic responses. These guidelines show the lower range of SSP required for sand-dominated river reaches across all ARIs. As such, it is likely that many rivers diversion channels won't allow sand deposition unless the river diversion dimensions, or subsequent growth of vegetation, can dissipate the hydraulic force of floods.

This study derived hydraulic thresholds in the absence of gauged data and should be treated accordingly. For example, we have compared frequent floods, encompassing the 2–5 yr ARI flows for ACARP and Pilbara hydraulic results, which can vary notably depending on the RFFE equation used (see supplemental tables S-2, S-3, and S-4). As with all modelling scenarios, an understanding and appreciation of the model's limitations are fundamental to their use. These modelled hydraulic guidelines represent the 25th-75th percentile of hydraulic conditions at the flood peak within the channel. A limitation is that this does not account for reduced hydraulic conditions associated with the rising and falling limb of the hydrograph nor a flow duration beyond the modelled 12 h flood. The hydraulic values should therefore be treated as upper thresholds of normal channel responses to floods. Additionally, overbank flood flows were identified through the hydrodynamic modelling of natural channels. Further modelling could be conducted to examine 10–20 year flood flows to improve the estimate of overbank flow occurrence within these channels.

Hydraulic conditions in diversion channels can be expected to deviate from the guideline values where local infrastructure affects the flow. Care must be taken to perform detailed analyses of infrastructure-related hydraulic impacts when performing detailed designs of the final river diversion landforms. Hydraulic modelling has been undertaken in the Marillana catchment. For example, the average maximum channel depth for a 100 year ARI flood event was 4.2 m, with an average cross-sectional velocity of 1.8 m/s (Rio Tinto 2010). Velocity increased to nearly 5 m/s at bridge crossings due to constriction of flows and alteration of the flow directions by bridge piers and embankments (Rio Tinto 2010). Within these modelled simulations, backwater development was noted to occur at confluences, contributing to the width of the floodplain (Rio Tinto 2010). An integrated hydrodynamic modelling approach is needed to ascertain the full extent of backwater flow conditions by modelling flow in the Marillana Creek relative to the influx of creek water from headwater channels.

Rogers and Davies (2016) demonstrated that there was an increase in runoff estimates in the Pilbara between ARR1987 and interim ARR2013 values. The design guidelines proposed here for the headwater channels assume minimal disturbance within the catchment. Catchment simulations were constructed with a variable Manning's n with depth to account for a full suite of native and appropriate vegetation within the catchment and channels. Clearing, fires, and construction, such as roads, pits, and associated mining infrastructure, will increase run-off rates within the catchment and decrease natural channel roughness. The occurrence of multiple flood events in quick succession can reduce runoff losses prompting an increase in runoff and peak flood flows in addition to backwater flow conditions within areas of pre-existing standing water such as pools. In addition, the performance of unvegetated river diversion channels will ultimately undergo different hydraulic conditions if appropriate roughness conditions are not considered within the channel design.

Conclusion

This research provides a series of geomorphic reference criteria for river diversions in the Pilbara. A range of hydraulic values are provided to emulate the hydraulic conditions experienced within headwater channels within the region. These can be compared against the existing condition of river diversion channels and to guide river restoration programs once mining has ceased. Broadly, this research highlights the diversity of reach types within headwater channels and has linked geomorphic features to the broader flooding conditions within the channel.

River restoration projects occasionally find little evidence for improved ecological outcomes (Bernhardt and Palmer 2011). However, using the established criteria, it is possible to create a river channel that has the best opportunity to replicate natural river conditions, and minimise excess erosion that could pose a risk to mine-related landforms and associated infrastructure. Additionally, these criteria are a means to improve current strategies relating to river diversion design and rehabilitation. These artificial channels

represent a significant river restoration challenge, and the associated guidelines represent a significant improvement in our understanding of channel heterogeneity in headwater river channels in the Pilbara. The presented geomorphic reference criteria represent a starting point for river diversion designs within the region and can be used as a benchmark to ensure channels that are most likely to replicate natural channel conditions.

Hydrodynamic modelling also highlighted the importance of overbank flows and the diversity of the channel-floodplain component within these headwater streams. Even frequently occurring (5 year ARI) flow events feature overbank flooding due to the heterogeneity in channel dimensions and stream bank heights as you move downstream. For river diversion channels, this highlights the necessity to consider channel-floodplain interactions for final river diversion designs within these semi-arid channels. Integrating these guideline hydraulic criteria should increase the likelihood of successful vegetation establishment and help the channel develop a characteristic range of geomorphic features. Once mining has ceased, there is more scope to create a channel that is both dynamic and stable. Reengaging the headwater channel with a floodplain for its final landform design will help recreate the overbank flow conditions identified with the flood modelling. Although this will not be feasible in every post-mining environment, integrating an appropriate range of hydraulic conditions will increase the likelihood that the river diversion will function as a natural headwater channel. Greater awareness of the reengagement of the channel with its floodplain and associated overbank flows are important in creating long-term, stable, post-mining landforms.

Supplementary Information The online version contains supplementary material available at https://doi.org/10.1007/s10230-023-00937-3.

Acknowledgements Funding for this project was provided by the University of Melbourne and a research grant awarded by BHP Billiton Ltd (Project 041639). We also thank Iain Rea at BHP for his enthusiasm for this project and Dr. Justin Stout and the 3RG group for their support. Lastly, we thank the anonymous reviewers for providing helpful feedback that improved the manuscript.

Funding Open Access funding enabled and organized by CAUL and its Member Institutions.

Data availability Data available on request from the authors.

References

Aryal SK, Silberstein RP, Fu G, Hodgson G, Charles SP, McFarlane D (2020) Understanding spatio-temporal rainfall-runoff changes in a semi-arid region. Hydrol Process 34:2510–2530. https://doi.org/10.1002/hyp.13744

Atkinson S, Markham A, Rafty M, Heyting M (2017) Pilbara creek diversions—Resilience gained through increased ore recovery and an integrated approach to design. Proc AusImm Iron Ore Conf, Perth, pp 367–374

Bernhardt ES, Palmer MA (2011) River restoration: the fuzzy logic of repairing reaches to reverse catchment scale degradation. Ecol Appl 21(6):1926–1931

Blanchette ML, Lund MA (2017) Biophysical closure criteria without reference sites: evaluating river diversions around mines. In: Wolkersdorfer C, Sartz L, Sillanpää M, Häkkinen A (eds) Proc. Mine Water and Circular Economy, IMWA Conf, Lappeenranta Finland, pp 437–444

BMT (2018) TUFLOW Classic / HPC User Manual Build 2018–03-AD. p 1–723. Accessed 2023–06–05, https://downloads.tuflow.com/_archive/TUFLOW/Releases/2018-03/TUFLOW%20Manual.2018-03.pdf

Brown RA, Pasternack GB (2014) Hydrologic and topographic variability modulate channel change in mountain rivers. J Hydrol 510:551–564. https://doi.org/10.1016/j.jhydrol.2013.12.048

Charles S, Fu G, McFarlane D, Hodgson G, Teng J, Barron O, Aryal S, Dawes W (2015) Hydroclimate of the Pilbara: past, present and future. Rep Govern West Aust Indust Part CSIRO Pilbara Water Res Assess CSIRO Land Water. https://doi.org/10.4225/08/584af1c180bda

Churchward HM, McArthur WM (1980) The soil pattern in relation to physiography and geology in the Northern Pilbara Region, Western Australia. CSIRO, Floreat Park, WA. Division of Land Resources Management. https://doi.org/10.4225/08/5ada38bd438bd

Conesa HM, Faz Á, Arnaldos R (2006) Heavy metal accumulation and tolerance in plants from mine tailings of the semiarid Cartagena–La Unión mining district (SE Spain). Sci Total Environ 366(1):1–11. https://doi.org/10.1016/j.scitotenv.2005.12.008

Cooke RU, Warren A, Goudie AS (1993) Desert Geomorphology. CRC Press London UK. https://doi.org/10.1201/b12557

Coppin NJ (2013) A framework for success criteria for mine closure, reclamation and post-mining regeneration. In: Tibbett M, Fourie AB, Digby C (eds) Mine Closure 2013, Proc, 8th International Seminar on Mine Closure. Australian Centre for Geomechanics, Cornwall, pp 485–493

Cowan WL (1956) Estimating hydraulic roughness. Coeff Agr Eng 37(7):473–475

Davies JR, Yip E (2014) Pilbara Regional Flood Frequency Analysis. Proc, 35th Hydrology and Water Resources Symp, Perth, Australia. pp 182–189. ISBN: 978–1–63439–935–7

Dogramaci S, Firmani G, Hedley P, Skrzypek G, Grierson P (2015) Evaluating recharge to an ephemeral dryland stream using a hydraulic model and water, chloride and isotope mass balance. J Hydrol 521:520–532. https://doi.org/10.1016/j.jhydrol.2014.12.017

Dragicevic S, Zivkovic N, Roksandic M, Kostadinov S, Novkovic I, Tosic R, Stepic M, Dragicevic M and Blagojevic B (2012) Land use changes and environmental problems caused by bank erosion:

a case study of the Kolubara River Basin in Serbia. Environmental Land Use Planning, pp 978–953
Erskine WD (2006) Review of the McArthur River Mine Open Cut Project Public Environmental Report. Accessed 2023–06–05, https://ntepa.nt.gov.au/__data/assets/pdf_file/0003/288084/rpt54_app3.pdf
Flatley A, Markham A (2021) Establishing effective mine closure criteria for river diversion channels. J Environ Manage 287:112287. https://doi.org/10.1016/j.jenvman.2021.112287
Flatley A, Rutherfurd I (2022) Comparison of regionalisation techniques for peak streamflow estimation in small catchments in the Pilbara. Austral Hydrol 9(10):165. https://doi.org/10.3390/hydrology9100165
Flatley A, Rutherfurd I, Hardie R (2018) River channel relocation: problems and prospects. Water 10(10):1360. https://doi.org/10.3390/w10101360
Flatley A, Rutherfurd I, Sims A (2022) Using structure-from-motion photogrammetry to improve roughness estimates for headwater dryland streams in the Pilbara. West Austra Remote Sens-Basel 14(3):454. https://doi.org/10.3390/rs14030454
Flavell D (2012) Design flood estimation in Western Australia. Aust J of Water Res 16(1):1–20. https://doi.org/10.7158/13241583.2012.11465400
Fryirs KA, Wheaton JM, Brierley GJ (2016) An approach for measuring confinement and assessing the influence of valley setting on river forms and processes. Earth Surf Proc Land 41(5):701–710. https://doi.org/10.1002/esp.3893
Gagen EJ, Levett A, Paz A, Gastauer M, Caldeira CF, da Silva Valadares RB, Bitencourt J, Alves R, Oliveira GR, Siqueira JO, Vasconcelos PM, Southam G (2019) Biogeochemical processes in canga ecosystems: armoring of iron ore against erosion and importance in iron duricrust restoration in Brazil. Ore Geol Rev 107:573–586. https://doi.org/10.1016/j.oregeorev.2019.03.013
Geoscience Australia (2015) Iron; fact sheet—Australian Atlas of Minerals Resources, Mines and Processing Centres. Accessed 2023–06–05, Iron | Geoscience Australia (ga.gov.au)
Grace D, McLeary M, Davies G (2014) Drainage principles and design for mine closure in the Pilbara. Proc, 35th Hydrology and Water Resources Symp, Perth, pp 94–100. ISBN: 978–1–63439–935–7
Hine A, Erskine PD (2016) Recognising and integrating stakeholder landform expectations into life-of-mine planning. Proc, AusIMM Life-of-Mine 2016 Conf, pp 154–157
James HL (1966) Chemistry of the Iron-rich sedimentary rocks, USGS Prof paper 440-W. US GPO. https://doi.org/10.3133/pp440W
Johnson SL, Wright AH (2003) Mine Void Water Resource Issues in Western Australia. Water and Rivers Commission, Hydrogeological Record Series, Report HG 9—Mine void water resource issues in Western Australia (dmp.wa.gov.au), Accessed 2023–06–05
Jowett IG (1998) Hydraulic geometry of New Zealand rivers and its use as a preliminary method of habitat assessment. Regul River 14(5):451–466. https://doi.org/10.1002/(SICI)1099-1646(199809)14:5%3c451::AID-RRR512%3e3.0.CO;2-1
Julien PY (1998) Erosion and Sedimentation. Camb Univ Press Cambridge UK. https://doi.org/10.1017/CBO9781139174107
Khademi H, Abbaspour A, Martínez-Martínez S, Gabarrón M, Shahrokh V, Faz A, Acosta JA (2018) Provenance and environmental risk of windblown materials from mine tailing ponds, Murcia, Spain. Environ Pollut 241:432–440. https://doi.org/10.1016/j.envpol.2018.05.084
Kneeshaw M, Morris RC (2014) The Cenozoic detrital iron deposits of the Hamersley Province. Western Australia Aust J Earth Sci 61(4):513–586. https://doi.org/10.1080/08120099.2014.898408
Knight DW, Shiono K (1996) River channel and floodplain hydraulics. In: Anderson MG, Walling DE, Bates PD (eds) Floodplain Processes. John Wiley and Sons Ltd, Chichester, UK, pp 139–181
Knighton DA, Nanson GC (2002) Inbank and overbank velocity conditions in an arid zone anastomosing river. Hydrol Proc 16(9):1771–1791. https://doi.org/10.1002/hyp.1076
Lamb D, Erskine PD, Fletcher A (2015) Widening gap between expectations and practice in Australian minesite rehabilitation. Ecol Manag Restor 16(3):186–195
Laurence D (2006) Optimisation of the mine closure process. J Clean Prod 14(3–4):285–298. https://doi.org/10.1016/j.jclepro.2004.04.011
Leopold LB, Maddock T, Jr (1953) The hydraulic geometry of stream channels and some physiographic implications. USGS Prof Paper 252, US GPO. https://doi.org/10.3133/pp252
Levett A, Gagen EJ, Gordon S (2019) Small but mighty: microorganisms offer inspiration for mine remediation and waste stabilisation. Microbiol Aust 40:190–194. https://doi.org/10.1071/MA19055
Li Z-X, Powell CM, Bowman R (1993) Timing and genesis of Hamersley iron-ore deposits. Explor Geophys 24(3–4):631–636. https://doi.org/10.1071/EG993631
McKenzie NL, Van Leeuwen S, Pinder AM (2009) Introduction to the Pilbara biodiversity survey, 2002–2007. Rec West Austral Museum Suppl 78(1):3–89
Pasternack GB, Hopkins CE (2017) Near-census 2D model comparison between SRH-2D and TUFLOW GPU for use in gravel/cobble rivers. Davis (CA), Univ of California at Davis, Prepared for Yuba County Water Agency. Accessed 2023–06–05, 2017-near-census-2d-model-comparison-between-srh-2d-and-tuflow-gpu-for-use-in-gravelcobble-rivers-pasternack-et-al-uc-davis-usa.pdf
Pepper M, Doughty P, Keogh JS (2013) Geodiversity and endemism in the iconic Australian Pilbara region: a review of landscape evolution and biotic response in an ancient refugium. J Biogeogr 40(7):1225–1239. https://doi.org/10.1111/jbi.12080
Rahman A, Haddad K, Zaman M, Ishak E, Kuczera G, Weinmann E (2012) Australian Rainfall and Runoff Revision Project 5: Regional Flood Methods: Stage 2 Report. P5/S2/015. p 1–349 https://researchdirect.westernsydney.edu.au/islandora/object/uws:29728 Accessed 2023–06–05
Ramanaidou ER, Morris RC, Horwitz RC (2003) Channel iron deposits of the Hamersley Province. Western Australia Aust J Earth Sci 50(5):669–690. https://doi.org/10.1111/j.1440-0952.2003.01019.x
Roche C, Judd S (2016) Ground truths: taking responsibility for Australia's mining legacies. Mineral Policy Institute. http://www.mpi.org.au/wp-content/uploads/2016/06/Ground-Truths-2016-web.pdf Accessed 2023–06–05
Rogers AD, Davies JR (2016) ARR 2015 Unpacked-Implications for stormwater design in WA. Proc, IPWEA State Conf, Fremantle, pp 1–12. Accessed 2023–06–05, https://www.jdahydro.com.au/images/publications/ARR2015Unpacked_IPWEA2016.pdf
Singh VP, Zhang L (2008) At-a-station hydraulic geometry relations, 1: theoretical development. Hydrol Process 22(2):189–215. https://doi.org/10.1002/hyp.6411
State of Queensland (2019) Guideline: Works that Interfere with Water in a Watercourse for a Resource Activity—Watercourse Diversions Authorised under the Water Act 2000. OSW/2019/4599. Dept of Natural Resources, Mines and Energy. Version 2.0. Accessed 2023–06–05, Guideline: Works that interfere with water in a watercourse for a resource activity—watercourse diversions authorised under the Water Act 2000 (daf.qld.gov.au)
Sutfin NA, Shaw JR, Wohl EE, Cooper DJ (2014) A geomorphic classification of ephemeral channels in a mountainous, arid region,

southwestern Arizona, USA. Geomorphology 221:164–175. https://doi.org/10.1016/j.geomorph.2014.06.005

Rio Tinto (2010) Resource Development: Marillana Creek regional flow balance and catchment hydrology. Appendix A9. Accessed 2023–06–05, https://www.epa.wa.gov.au/sites/default/files/PER_documentation/Appendix%20A9%20-%20Marillana%20Creek%20Regional%20Flow%20Balance.pdf

Tooth S, Nanson GC (1999) Anabranching rivers on the Northern Plains of arid central Australia. Geomorphology 29(3–4):211–233. https://doi.org/10.1016/S0169-555X(99)00021-5

van Zyl Dirk JA, Straskraba, V (1999) Mine closure considerations and semi-arid areas. Proc, Mine Water and Environment, IMWA Congress, Sevilla, pp 213–220. Accessed 2023–06–05, https://www.imwa.info/docs/imwa_1999/IMWA1999_vanZylDirk_213.pdf

Verboom WH, Pate JS (2006) Evidence of active biotic influences in pedogenetic processes. Case studies from semiarid ecosystems of south-west Western Australia. Plant Soil 289(1):103–121. https://doi.org/10.1007/s11104-006-9075-6

White K, Hardie R (2000) Maintenance of Geomorphic Processes in Bowen Basin River Diversions. ACARP Project C8030_C9068. https://acarp.com.au/abstracts.aspx?repId=C8030_C9068 Accessed 2023–06–05

White K, Hardie R, Lucas R, Merritt J, Kirsch B (2014a) The evolution of watercourse diversion design in central Queensland coal mines. In: Vietz G, Rutherfurd ID, Hughes R (eds) Proc, 7th Australian Stream Management Conf. Townsville, Australia, pp 238–248

White K, Lucas R, Hardie R, Moar D, Blackham D (2014b) Criteria for Functioning River Landscape Units in the Mining and Post Mining Landscapes. Report prepared for ACARP Project C, 20017

Williams GB (1922) Flood discharges and the dimensions of spillways in India. Engineering (london) 134(9):321–322